

Chapter 2

Experimental Anion Affinities for the Air–Water Interface*

*This chapter is reproduced with permission from J. Cheng, C. D. Vecitis, M. R. Hoffmann, and A. J. Colussi, *Journal of Physical Chemistry B*, **2006**, *110*, 25598. Copyright © 2006, American Chemical Society

2.1 Abstract

Anion affinities, γ_X , for the aerial interface of aqueous ($\text{Br}^- + \text{NO}_3^- + \text{I}^- + \text{SCN}^- + \text{BF}_4^- + \text{ClO}_4^-$) solutions are determined by electrospray ionization-mass spectrometry. The composition of the ions ejected from the surface of fissioning nanodroplets shows that γ_X 's increase (decrease) exponentially with anionic radii, a_X (dehydration free energies, dG_X), and selectively respond to the presence of surfactants. BF_4^- , the least hydrated and polarizable anion of the set, has one of the largest γ_X 's. Non-ionic surfactants decrease γ_I and γ_{SCN} , but increase γ_{BF_4} . Cetyltrimethyl ammonium markedly enhances the γ_X 's of smaller anions over those of larger ones. A similar, but weaker effect is observed upon lowering the pH of the bulk solutions from 8.2 to 3.0. Dodecyl sulfate has a negligible effect on γ_X 's. Considering that: (1) universal many-body electrodynamic interactions will progressively stabilize the interfacial layer as its dielectric permittivity falls relative to that of the bulk solution, (2) water permittivity is uniformly depressed by increasing concentrations of these anions, we infer that the observed Hofmeister correlation: $\ln \gamma_X \propto -{}^dG_X$, is consistent with the *optimal depression of the permittivity of the drier interfacial layer by the least hydrated ions*. Ion-ion interactions can significantly influence γ_X 's in environmental aqueous media.

2.2 Introduction

Few phenomena are more ubiquitous, or have been more investigated, than those induced by the dissimilar propensities of anions for aqueous interfaces.¹⁻⁴ Fundamental biochemical, technological and environmental processes are driven by the selective affinities of the various anions for the interfaces involved. They are labeled “Hofmeister effects” (HEs) after observations made 118 years ago.⁵⁻⁶ Explanations abound. They range from those based on continuum,⁷⁻¹³ or heuristic molecular models,¹⁴ to non-primitive molecular dynamic simulations.¹⁵⁻¹⁸ However, “*HEs remain a mystery after more than 100 years*”,¹⁰ “*perhaps the only thing certain about HEs is that we do not understand the physical basis for the process*”,¹⁹ “*simulations that confirm intuitions should be considered tautological*”.¹¹

Hofmeister correctly linked anion propensities for the boundaries between water and less polar media with the ‘water withdrawing power’ of anions, an unquantified property at the time.²⁰ It has been recently argued, however, that anion polarizability is the most important factor determining HEs at air/electrolyte solution interfaces.^{18,21-22} The argument rests on molecular dynamic (MD) calculations in which anions accumulate in the outermost layer after their polarizabilities are turned on in the models, and on similarly interpreted surface-sensitive experiments.²³ Thus, it has been alleged that halide anion propensities are proportional to their polarizabilities.²⁴ Notice that the negative surface potentials measured over (most) electrolyte solutions ~50 years ago themselves require anions to be closer than cations to the interface.²⁵⁻²⁷

The affinities of the heavier halide anions for aerosol interfaces play important roles in atmospheric chemistry.^{2,28-36} The same tendencies underlie the fact that the saline aerosol (up to $\sim 10^4$ Tg/yr) incessantly released by the oceans is highly (10 to 10^4 times) enriched in

bromide and iodide.^{32,37} Considering that these huge enrichment factors cannot be accounted for by the modest differential Cl⁻/Br⁻/I⁻ concentration gradients predicted for the interfacial region, we decided to reinvestigate the mechanism of anion fractionation during the aerosolization of electrolyte solutions.^{33,38-43} In this chapter we report experiments on the simultaneous detection of Br⁻, NO₃⁻, I⁻, SCN⁻, BF₄⁻ and ClO₄⁻ at the aerial interface of sub-millimolar aqueous binary solutions via electrospray ionization-mass spectrometry^{40,44-48} in the presence or absence of surfactants and urea.^{31,49-55} The results are analyzed in terms of fundamental concepts and new information.

2.3 Experimental Section

An electrospray ionization mass spectrometer (HP-1100 MSD) with an atmospheric pressure ionization interface of orthogonal geometry was used in this study. Electrolyte solutions (50 $\mu\text{L min}^{-1}$) were pumped into the spraying chamber through a grounded stainless steel needle injector (100 μm bore). Continuous flow conditions minimize contamination by spurious tensioactive species, which often compromises static experiments. Instrumental parameters (drying gas flow: 10 L min^{-1} ; drying gas temperature: 250 $^{\circ}\text{C}$; nebulizer pressure: 35 psi; collector capillary voltage: 1.5 kV; fragmentor voltage: 80 V) were chosen to optimize mass signals with minimal ion fragmentation. Mass spectra were acquired at preset m/z values: 58 and 60 (^{32,34}SCN⁻), 62 (NO₃⁻), 79 and 81 (Br⁻), 86 and 87 (^{10,11}BF₄⁻), 99 and 101 (^{35,37}ClO₄⁻) and 127 (I⁻). Reported data are the average of at least duplicate experiments.

Pure (98% purity or higher) NaBr, NaI, NaNO₃, NaClO₄, NaBF₄ and NaSCN (EM science or Sigma-Aldrich), Triton X-114 and cetyltrimethyl ammonium chloride (CTAC, Sigma-Aldrich), sodium dodecylsulfate (SDS, Bio-Rad) and urea (Mallinckrodt) were used as received. Equimolar binary solutions were prepared in MilliQ water or D₂O (Cambridge

Isotopes) with and without surfactants or urea. The use of senary solutions substantially reduces experimental dispersion, and the possible effect of potential impurities on present measurements. The pH of senary solutions, initially at 6.5, was adjusted by addition of 1 mM NaOH or HCl at constant ionic strength, and measured with a calibrated pH meter.

2.4 Results and Discussion

Figure 2.1 shows a negative ion mass spectrum of electrosprayed salt solutions. From this information, normalized anion affinities, f_{X^-} , were calculated from the sum of ion counts, $I_{m/z}$, for the isotopic variants of each anionic species (e.g., $(I_{58} + I_{60})$ for SCN^- , etc.) and the total ion count:

$$f_{X^-} = \frac{\sum I_{m/z}}{\sum I_{m/z}} \quad (2.1)$$

Relative anion affinities, γ_{X^-} , are defined as multiples of f_{Br^-} , the value for the least enriched anion at the interface in the absence of surfactants: $\gamma_{X^-} = f_{X^-}/f_{\text{Br}^-}$ (table 2.1). γ_{X^-} s measured in H_2O or D_2O are identical within experimental error.

Droplets generated during breakup of the liquid jet issuing from the grounded nozzle are spontaneously charged via microscopic fluctuations. The subsequent, uneven shedding of mass and charge by electrosprayed droplets forces the anions present at the air/water interface to preferentially carry most of the excess charge into offspring droplets.⁵⁶ Individual anions are ultimately ejected into the gas-phase via field desorption from negatively charged nanodroplets.^{40,45-46,57-63} Therefore, the relative anion abundances registered by the mass spectra (figure 2.1) reflect the anion distribution in the ensemble of single-ion water clusters ejected from the surface of disintegrating nanodroplets.⁵⁷⁻⁵⁸ In the orthogonal geometry

employed in these experiments the instrument samples the nanodroplets ejected laterally from the electrosprayed jet. There is conclusive evidence that tensioactive species tend to accumulate in the periphery of the conical mist created ahead of the inlet orifice.⁴⁸ Considering that the relative anion signals obtained by spraying solutions doped with 10 μM SDS (anionic) or CTAC (cationic) surfactants are identical within experimental error, we conclude that the basic mechanism of anion enrichment does not involve ion-ion interactions.

Figures 2.2 to 2.4 show semilogarithmic plots of f_X as a function of the aqueous anionic radius, a_X , free energy of dehydration dG_X , and polarizability α_X , respectively.⁶⁴ It is apparent that anion affinities for the air/water interface are strongly correlated with anionic radii: $\ln f_X \propto a_X$ ($R^2 = 0.96$), and free energies of dehydration: $\ln f_X \propto {}^dG_X$ ($R^2 = 0.91$), in full accord with Hofmeister's analysis,²⁰ and Monte Carlo calculations.^{15,65} However, there is no discernible correlation between f_X 's and anion polarizabilities α_X 's (Figure 2.4).^{3,7,18,21,66-67} Tetrahedral BF_4^- , which has the smallest dehydration free energy of this set of anions, but is approximately 2.75 times less polarizable than iodide (table 2.1), provides a fair test of the relative importance of anion polarizability versus anion dehydration energy in the mechanism of interfacial enrichment. Although the reported anion affinities depend to a certain extent on instrumental settings, these correlations are robust: f_X 's measured at 3 kV capillary voltage still increase exponentially with a_X . f_X 's measured in the 10 μM to 10 mM concentration range are identical within experimental error.

Surfactants significantly affect f_X 's. All surfactants uniformly depress the total anion count at concentrations below their critical micellar concentrations.⁶⁸⁻⁶⁹ Since nonionic surfactants do not displace anions from the interface at these concentrations (a weak

attraction might be even expected) this finding suggests that surfactants compete with anions in decreasing surface energy. Urea (Figure 2.5), a water structure-breaker,⁵² and Triton X-114 (Figures 2.7 and 2.8), a non-ionic polyether amphiphile, comparably, slightly, but selectively influence f_X 's. The interfacial layer becomes more populated by the least hydrated BF_4^- at the expense of the more polarizable I^- and SCN^- anions upon addition of urea or Triton X-114. The devaluation of the comparative advantage of I^- and SCN^- over BF_4^- (BF_4^- , having the smallest dG_X , is indeed underrepresented at the interface, cf. Figure 2.3) further suggests that the more polarizable anions are somewhat more efficient in stabilizing the interfacial layer.⁷⁰⁻

71

While the anionic dodecylsulfate indiscriminately repels all anions from the interface, as expected from electrostatics, f_X 's are quite sensitive to the cationic amphiphile cetyltrimethylammonium (Figure 2.6).⁷²⁻⁷³ The smallest (and least enriched in the absence of additives) anions, NO_3^- and Br^- , are specifically enhanced several fold. As a result, the f_X 's measured in the presence of 1 mM CTAC no longer correlate with anion radii or dehydration free energies. Positive headgroups seem to attract the smaller anions into closer contact, and induce significant changes in their orientation and solvation at the interface.⁷⁴ It is well known that ion charges *and* radii both affect ion distributions near interfaces.⁷⁵ We also found that $\gamma_{\text{NO}_3^-}$ increases 2.3 times, respectively, while most γ_X 's remain nearly constant as the pH of the bulk solutions is lowered from 8.2 to 3.0. The onset of $\gamma_{\text{NO}_3^-}$ increases occurs at about pH 4.0, suggesting that the interface becomes positively charged via proton adsorption under acidic conditions.⁴ In this context, it is relevant to point out that the marine aerosol, which is generated during bubble bursting at the ocean surface, consists of positively charged

droplets.^{39,76}

Much of the current literature focuses on the width of the interfacial region.⁷⁷ However, since even surface-sensitive spectroscopies collect signals from interfacial slabs of $\delta \approx 1.0$ nm thicknesses,²³ the fine-grained interfacial concentration profiles obtained by MD calculations, if they were consequential, represent an authentic challenge.¹⁸ Anions are effectively enriched in the layers probed in our experiments because the combined ClO_4^- ($m/z = 99$ and 101) signals are only 2.5 times smaller than the $m/z = 265$ signal of the SDS surfactant in equimolar $10 \mu\text{M}$ solutions. Assuming that SDS is bound to a $\delta \approx 0.3$ nm outermost layer, we tentatively infer that ClO_4^- ions are sampled from $\delta \approx 1.0$ nm interfacial sections that are smaller than the estimated ≈ 2.5 nm radii of fissioning droplets,⁵⁷⁻⁵⁸ On the other hand, surface tension measurements involve integral concentration profiles. The possibility that different interactions dominate at various depths, i.e., that the results obtained by different techniques could not be comparable, cannot be dismissed at this time.²³

A physically meaningful interpretation of interfacial anion affinities should be based on an energy balance between opposing effects, rather than on simply correlating affinities with specific ion properties. Since anions *are* polarizable, the finding that some anions become enriched at the interface after their polarizabilities are included in MD calculations strictly shows that a deficiency has been corrected, not that anion enrichments should correlate with anion polarizabilities. While it is easy to envision that water density decreases smoothly toward the interface, the factors that determine the concentration profiles of cations and anions in the boundary layer are not immediately apparent. The sizable dehydration free energies of most ions, in conjunction with lower water density at the interface, will draw them into the bulk.^{9,15,65} Image charge repulsion will enhance this tendency. This drive would

be ultimately balanced by the entropy losses associated with ion confinement into a reduced volume. Hence, large dehydration free energies conspire against significant interfacial ion excesses. The preferential stabilization of the more polarizable anions in the strong electric field at the interface would, in principle, contribute to mitigate the adverse energy balance. Figure 2.4 shows, however, that this contribution is at best minor. Clearly, the major interactions remain to be identified that draw anions toward the interface and offset their aversion for this drier medium. Notice that if these were the only interactions involved, the solution bulk would be separated from air by a more dilute layer.

The thermodynamic stability of a contiguous three-layer macroscopic array cannot be exclusively analyzed in terms of localized ion-water interactions. Macroscopic phases in contact are mutually stabilized via collective dispersive interactions arising from density and orientation fluctuations over the entire system.⁷⁸⁻⁸⁰ By properly accounting for the global, many-body electrodynamic interactions among three contiguous phases, it is possible to infer that the central layer is stabilized when its overall (i.e., dispersive and orientational) polarizability lies between those of the bulk solution and air.⁷⁸⁻⁷⁹ This powerful criterion shifts the focus from ion polarizabilities to ion effects on the polarizability of water as a macroscopic medium. The broad temporal scales of many-body interactions in dielectric water are presumably better captured by Monte Carlo than by Molecular Dynamic calculations. The large difference between the dielectric permittivities of water and air, due to the unique properties of water as a hydrogen-bonded solvent, tends to amplify the effects of perturbations to water dynamics. Since electrolytes, as a rule, decrease the dielectric permittivity of water,⁸¹⁻⁸⁴ *aqueous layers separating electrolyte solutions from air are expected to be stabilized by excess ion concentrations.* Anions largely achieve this effect in

the bulk by shortening the range and slowing down water dipolar correlations. From this perspective, we propose that the rival factors controlling ion affinities for the air/water interface appear to be: (1) ion dehydration energies and (2) nonlocal stabilization energies resulting from the depression of interfacial water permittivity by local ion excesses.⁹

Since the concentration dependences of the static permittivities and relaxation times of water in NaBr, NaI, NaNO₃, NaClO₄ and NaSCN solutions are nearly independent of the nature of the anion,⁸⁵⁻⁸⁶ *anion affinities largely reflect differences in dehydration free energies*. Considering that the dehydration energies of anions are considerably smaller than those of cations, this analysis naturally accounts for the negative (relative to the bulk) surface potentials measured long ago.²⁶⁻²⁷ The Jones-Ray effect,⁸⁷ i.e., the lower surface tensions of dilute aqueous electrolyte solutions, also follows from this analysis and the Gibbs isotherm. This view readily allows for variations of anion affinities when air is replaced by other media, such as hydrophobic membranes or proteins.^{1,11,20} If for no other reason, anions, particularly in the ~1 M model solutions used in MD simulations, *must* be polarizable to relay (rather than shield) electrodynamic interactions over the entire molecular ensemble.

Summing up, the Hofmeister series of anion affinities for the air/water interface is paradoxically realized by the nonspecific effect of anions on the dielectric properties of interfacial water. Under realistic environmental conditions, surfactants may decisively affect anion affinities. The huge anion enrichments found in the finest marine aerosol likely result from the amplification of relative anion affinities in successive droplet fission events.^{39,47} Further work is underway.

2.5 Acknowledgments

This work was financed by NSF grant ATM-0534990.

2.6 References

- (1) Kunz, W. *Pure Appl. Chem.* **2006**, *78*, 1611.
- (2) Lewis, E. R.; Schwartz, S. E. *Sea Salt Aerosol Production: Mechanisms, Methods, Measurements and Models – A Critical Review*; American Geophysical Union: Washington, DC, 2004; Geophysical Monograph, Vol. 152.
- (3) Ghosal, S.; Hemminger, J. C.; Bluhm, H.; Mun, B. S.; Hebenstreit, E. L. D.; Ketteler, G.; Ogletree, D. F.; Requejo, F. G.; Salmeron, M. *Science* **2005**, *307*, 563.
- (4) Pegram, L. M.; Record, M. T. *Proc. Nat. Acad. Sci. U.S.A.* **2006**, *103*, 14278.
- (5) Hofmeister, F. *Arch. Exp. Pathol. Pharmacol. (Leipzig)* **1888**, *24*, 247.
- (6) Gurau, M. C.; S.M., L.; Castellana, E. T.; Albertorio, F.; Kataoka, S.; Cremer, P. S. *J. Am. Chem Soc.* **2004**, *126*, 10522.
- (7) Bondesson, L.; Frediani, L.; Agren, H.; Mennucci, B. *J. Phys. Chem. B* **2006**, *110*, 11361.
- (8) Edwards, S. A.; Williams, D. R. M. *Europhys. Lett.* **2006**, *74*, 854.
- (9) Bostrom, M.; Kunz, W.; Ninham, B. W. *Langmuir* **2005**, *21*, 2619.
- (10) Bostrom, M.; Ninham, B. W. *Langmuir* **2004**, *20*, 7569.
- (11) Kunz, W.; Lo Nostro, P.; Ninham, B. W. *Curr. Opin. Colloid Interface Sci.* **2004**, *9*, 1.
- (12) Zhou, H. X. *Proteins* **2005**, *61*, 69.
- (13) Frediani, L.; Mennucci, B.; Cammi, R. *J. Phys. Chem. B* **2004**, *108*, 13796.
- (14) Dill, K. A.; Truskett, T. M.; Vlachy, V.; Hribar-Lee, B. *Annu. Rev. Biophys. Biomol. Struct.* **2005**, *34*, 173.
- (15) Hagberg, D.; Brdarski, S.; Karlstrom, G. *J. Phys. Chem. B* **2005**, *109*, 4111.

- (16) Wilson, M. A.; Pohorille, A. *J. Chem. Phys.* **1991**, *95*, 6005.
- (17) Cacace, M. G.; Landau, E. M.; Ramsden, J. J. *Quarterly Rev. Biophys.* **1997**, *30*, 241.
- (18) Jungwirth, P.; Tobias, D. J. *Chem. Rev.* **2006**, *106*, 1259.
- (19) Bowron, D. T.; Finney, J. L. *J. Chem. Phys.* **2003**, *118*, 8357.
- (20) Kunz, W.; Henle, J.; Ninham, B. W. *Curr. Opin. Colloid Interface Sci.* **2004**, *9*, 19.
- (21) Petersen, P. B.; Saykally, R. J. *Annu. Rev. Phys. Chem.* **2006**, *57*, 333.
- (22) Jungwirth, P.; Tobias, D. J. *J. Phys. Chem. B* **2002**, *106*, 6361.
- (23) Petersen, P. B.; Saykally, R. J. *J. Phys. Chem. B* **2006**, *110*, 14060.
- (24) Knipping, E. M.; Lakin, M. J.; Foster, K. L.; Jungwirth, P.; Tobias, D. J.; Gerber, R. B.; Dabdub, D.; Finlayson-Pitts, B. J. *Science* **2000**, *288*, 301.
- (25) Randles, J. E. B. *Discuss. Faraday Soc.* **1957**, *24*, 194.
- (26) Jarvis, N. L. *J. Geophys. Res.* **1972**, *77*, 5177.
- (27) Jarvis, N. L.; Scheiman, M. A. *J. Phys. Chem.* **1968**, *72*, 74.
- (28) McFiggans, G. *Nature* **2005**, *433*, E13.
- (29) O'Dowd, C. D.; Jimenez, J. L.; Bahreini, R.; Flagan, R. C.; Seinfeld, J. H.; Hameri, K.; Pirjola, L.; Kulmala, M.; Jennings, S. G.; Hoffmann, T. *Nature* **2002**, *417*, 632.
- (30) Carpenter, L. J. *Chem. Rev.* **2003**, *103*, 4953.
- (31) Liss, P. S.; Duce, R. A. *The Sea Surface and Global Change*; Cambridge University Press: Cambridge, UK, 1997.
- (32) Duce, R. A.; Hoffman, E. J. *Ann. Rev. Earth Planet. Sci.* **1976**, *4*, 187.
- (33) Macintyre, F. *Tellus* **1970**, *22*, 451.
- (34) Sander, R.; Keene, W. C.; Pszenny, A. A. P.; Arimoto, R.; Ayers, G. P.; Baboukas, E.; Cainey, J. M.; Crutzen, P. J.; Duce, R. A.; Honninger, G.; Huebert, B. J.; Maenhaut, W.;

- Mihalopoulos, N.; Turekian, V. C.; Van Dingenen, R. *Atmos. Chem. Phys.* **2003**, *3*, 1301.
- (35) Finlayson-Pitts, B. J. *Chem. Rev.* **2003**, *103*, 4801.
- (36) Garrett, B. C. *Science* **2004**, *303*, 1146.
- (37) Boyce, S. G. *Science* **1951**, *113*, 620.
- (38) Macintyre, F. J. *Phys. Chem.* **1968**, *72*, 589.
- (39) Blanchard, D. C. *Prog. Oceanogr.* **1963**, *1*, 71.
- (40) Lin, S. P.; Reitz, R. D. *Ann. Rev. Fluid Mech.* **1998**, *30*, 85.
- (41) Leifer, I.; de Leeuw, G.; Cohen, L. H. *Geophys. Res. Lett.* **2000**, *27*, 4077.
- (42) Blanchard, D. C.; Syzdek, L. D. *Limnol. Oceanogr.* **1978**, *23*, 389.
- (43) Duchemin, L.; Popinet, S.; Josserand, C.; Zaleski, S. *Phys. Fluids* **2002**, *14*, 3000.
- (44) Yamashita, M.; Fenn, J. B. *J. Phys. Chem.* **1984**, *88*, 4451.
- (45) Fenn, J. B. *Angew. Chem. Int. Ed.* **2003**, *42*, 3871.
- (46) Fenn, J. B. *J. Am. Soc. Mass Spectrom.* **1993**, *4*, 524.
- (47) Cech, N. B.; Enke, C. G. *Anal. Chem.* **2001**, *73*, 4632.
- (48) Tang, K. Q.; Smith, R. D. *J. Am. Soc. Mass Spectrom.* **2001**, *12*, 343.
- (49) Liu, X.; Duncan, J. H. *Nature* **2003**, *421*, 520.
- (50) Quinn, J. A.; Steinbrook, R. A.; Anderson, J. L. *Chem. Eng. Sci.* **1975**, *30*, 1177.
- (51) Stepanets, O. V.; Soloveva, G. Y.; Mikhailova, A. M.; Kulapin, A. I. *J. Anal. Chem.* **2001**, *56*, 290.
- (52) Franks, F. *Water, a Comprehensive Treatise*; New York: Plenum Press, 1975; Vol. 4.
- (53) Ohmine, I. *J. Phys. Chem.* **1995**, *99*, 6767.
- (54) Siu, D.; Koga, Y. *J. Phys. Chem. B* **2005**, *109*, 16886.
- (55) Frinak, E. K.; Abbatt, J. P. D. *J. Phys. Chem. A* **2006**, *110*, 10456.

- (56) Enke, C. G. *Anal. Chem.* **1997**, *69*, 4885.
- (57) Consta, S. *Theor. Chem. Acc.* **2006**, *116*, 373.
- (58) Ichiki, K.; Consta, S. *J. Phys. Chem. B* **2006**, *110*, 19168.
- (59) Rohner, T. C.; Lion, N.; Girault, H. H. *Phys. Chem. Chem. Phys.* **2004**, *6*, 3056.
- (60) Cech, N. B.; Enke, C. G. *Mass Spectrom. Rev.* **2001**, *20*, 362.
- (61) Iribarne, J. V.; Dziedzic, P. J.; Thomson, B. A. *Int. J. Mass Spectrom. Ion Processes* **1983**, *50*, 331.
- (62) Iribarne, J. V.; Thomson, B. A. *J. Chem. Phys.* **1976**, *64*, 2287.
- (63) Znamenskiy, V.; Marginean, I.; Vertes, A. *J. Phys. Chem. A* **2003**, *107*, 7406.
- (64) Marcus, Y. *Ion Properties*; Marcel Dekker: New York, 1997.
- (65) Karlstrom, G.; Hagberg, D. *J. Phys. Chem. B* **2002**, *106*, 11585.
- (66) Weber, R.; Winter, B.; Schmidt, P. M.; Widdra, W.; Hertel, I. V.; Dittmar, M.; Faubel, M. *J. Phys. Chem. B* **2004**, *108*, 4729.
- (67) Chang, T. M.; Dang, L. X. *Chem. Rev.* **2006**, *106*, 1305.
- (68) Hernainz, F.; Calero, M.; Blazquez, G.; Caro, A. *J. Chem. Eng. Data* **2006**, *51*, 1216.
- (69) Chang, H. C.; Hwang, B. J.; Lin, Y. Y.; Chen, L. J.; S.Y., L. *Rev. Sci. Instr.* **1998**, *69*, 2514.
- (70) Schrodle, S.; Hefter, G.; Kunz, W.; Buchner, R. *Langmuir* **2006**, *22*, 924.
- (71) Fernandez, P.; Schrodle, S.; Buchner, R.; Kunz, W. *ChemPhysChem.* **2003**, *4*, 1065.
- (72) Ryhanen, S. J.; Saily, V. M. J.; Kinnunen, P. K. J. *J. Phys. Condens. Matter* **2006**, *18*, S1139.
- (73) Baar, C.; Buchner, R.; Kunz, W. *J. Phys. Chem. B* **2001**, *105*, 2906.
- (74) Benderskii, A. V.; Henzie, J.; Basu, S.; Shang, X.; Eisenthal, K. B. *J. Phys. Chem. B*

2004, *108*, 14017.

(75) Luo, G.; Malkova, S.; Yoon, J.; Schultz, D. J.; Lin, B.; Meron, M.; Benjamin, I.; Vanysek, P.; Schlossman, M. L. *Science* **2006**, *311*, 216

(76) Blanchard, D. C. *J. Meteor.* **1958**, *15*, 383.

(77) Deutsch, M. *Faraday Discuss.* **2005**, *129*, 89.

(78) Israelachvili, J. *Intermolecular & Surface Forces*, 2nd ed.; Academic Press: London, 1992.

(79) Dzyaloshinskii, I.E.; Lifshitz, E. M.; Pitaevskii, L. P. *Adv. Phys.* **1961**, *10*, 165.

(80) Wilen, L. A.; Wettlaufer, J. S.; Elbaum, M.; Schick, M. *Phys. Rev. B* **1995**, *52*, 12426.

(81) Kaatze, U. *J. Solut. Chem.* **1997**, *26*, 1049.

(82) Barthel, J.; Buchner, R. *Pure Appl. Chem.* **1991**, *63*, 1473.

(83) Hildebrandt, A.; Blossey, R.; Rjasanow, S.; Kohlbacher, O.; Lenhof, H. P. *Phys. Rev. Lett.* **2004**, *93*, 108104.

(84) Gavryushov, S.; Linse, P. *J. Phys. Chem. B* **2003**, *107*, 7135.

(85) Wachter, W.; Kunz, W.; Buchner, R.; Hefter, G. *J. Phys. Chem. A* **2005**, *109*, 8675.

(86) Koga, Y.; Westh, P.; Davies, J. V.; Miki, K.; Nishikawa, K.; Katayanagi, H. *J. Phys. Chem. A* **2004**, *108*, 8533.

(87) Petersen, P. B.; Saykally, R. J. *J. Am. Chem Soc.* **2006**, *127*, 15446.

Table 2.1 Interfacial affinities and molecular properties of anions

Anion X⁻	Normalized Affinities^a f_{X^-}^b	Relative Affinities^a γ_{X^-}^b	Radii^c $a_{X^-} \times 10^{12}$ /m	Dehydration Free Energies^c ^dG_{X⁻}/ kJ mol⁻¹	Polarizabilities^c $\alpha_{X^-} \times 10^{30}$ /m³
Br⁻	0.023	1.00	196	321	4.99
NO₃⁻	0.033	1.40	206 ^d	306	4.20
I⁻	0.090	3.85	220	283	7.65
SCN⁻	0.098	4.17	213	287	6.86
BF₄⁻	0.301	12.86	230	200	2.78
ClO₄⁻	0.455	19.45	240	214	4.92

^a See text for definition

^b This work

^c Reference 60

^d Equatorial radius

Figure 2.1. ESI-MS of a 100 μM aqueous solution of the sodium salts of each of the following anions: SCN^- , NO_3^- , Br^- , BF_4^- , ClO_4^- and I^- , at pH 6.5. Ion signal intensities normalized to the total ion intensity: $\sum I_i = 1$. $I_{\text{SCN}^-} = 0.097$, $I_{\text{NO}_3^-} = 0.033$, $I_{\text{Br}^-} = 0.023$, $I_{\text{BF}_4^-} = 0.301$, $I_{\text{ClO}_4^-} = 0.455$, $I_{\text{I}^-} = 0.090$.

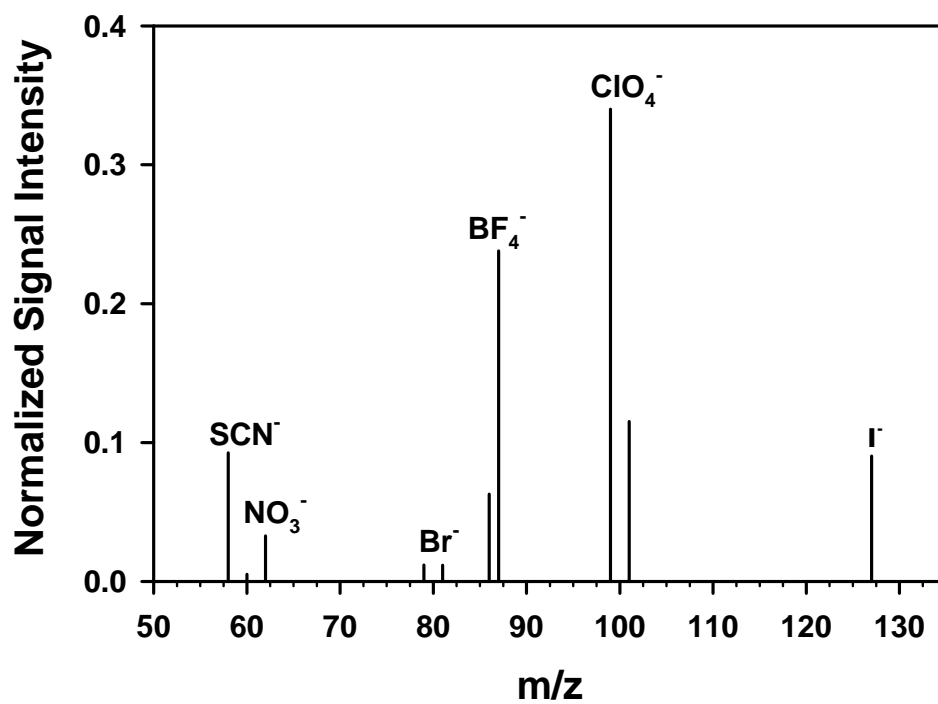


Figure 2.2. Symbols: Normalized anion affinities, f_X^- , versus anionic radii, a_X^- , from Reference 60. Solid line: linear regression: $\ln f_X^- \propto a_X^-$ ($R^2 = 0.956$).

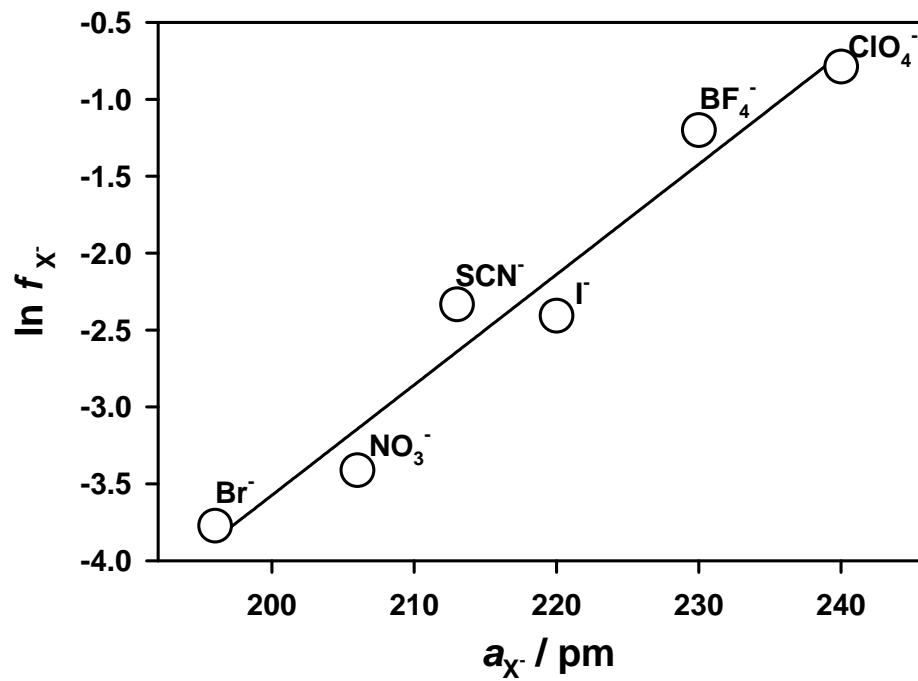


Figure 2.3. Symbols: Normalized anion affinities, f_X^- , versus free energies of anion dehydration, ${}^dG_{X^-}$, from Ref. 60. Solid line: linear regression: $\ln f_X^- \propto {}^dG_{X^-}$ ($R^2=0.910$).

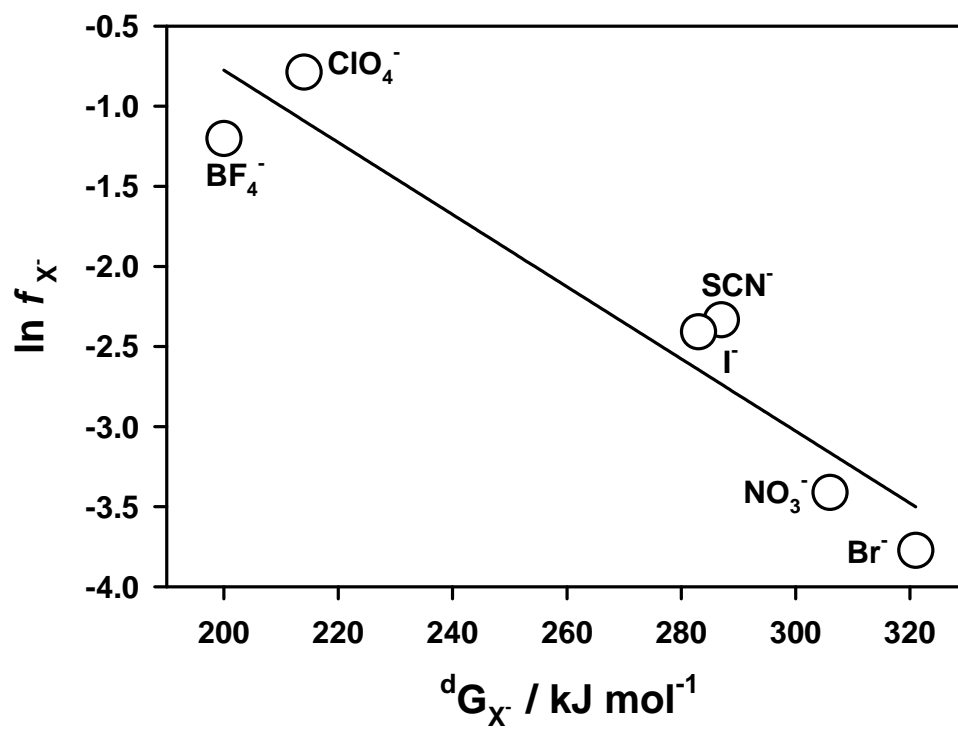


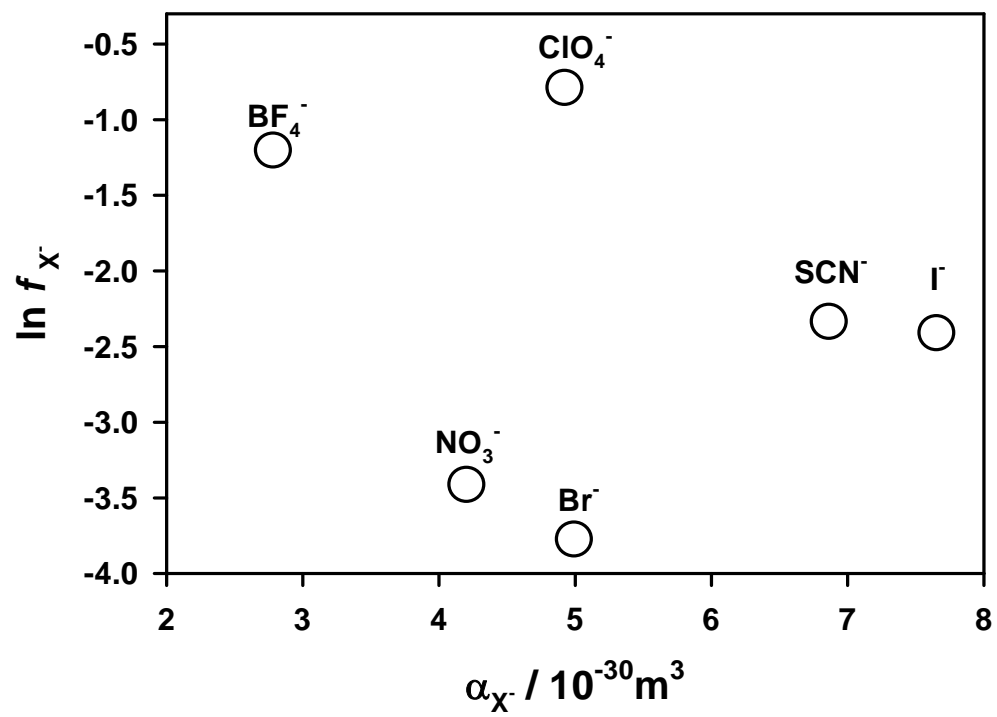
Figure 2.4. Normalized anion affinities, f_X^- , versus anion polarizabilities, α_X^- , from Ref. 60.

Figure 2.5. Symbols: Ratios of normalized anion affinities, $f_X/f_X(0)$, as function of urea concentration. ■(BF_4^-); ◇(NO_3^-); ▽(ClO_4^-); □(Br^-); ○(I^-); △(SCN^-). $[\text{X}_i^-] = 0.1 \text{ mM}$.

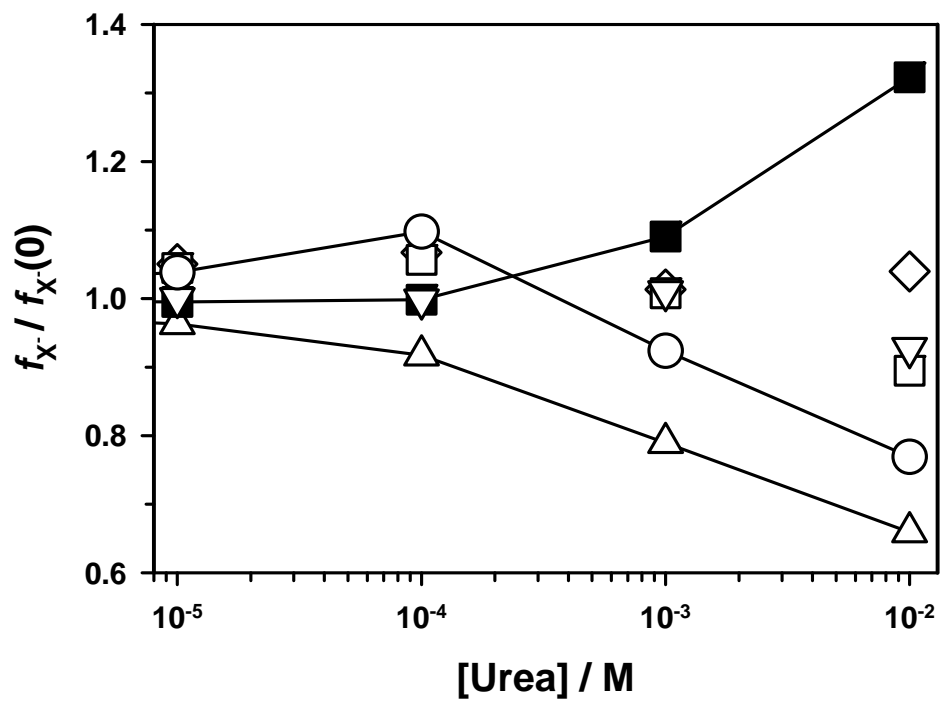


Figure 2.6. Symbols: Ratios of normalized anion affinities, $f_x/f_x(0)$, as function of cetyltrimethyl ammonium chloride (CTAC) concentration. ■(BF_4^-); ◇(NO_3^-); ▽(ClO_4^-); □(Br^-); ○(I^-); △(SCN^-). $[\text{X}_i^-] = 0.1 \text{ mM}$.

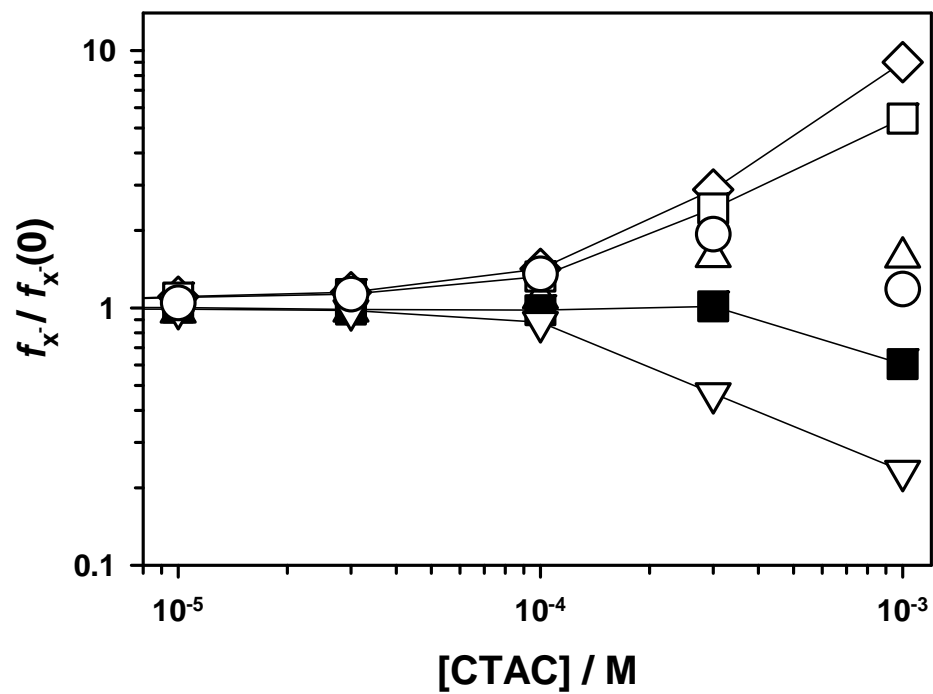


Figure 2.7. Symbols: Ratios of normalized anion affinities, $f_{X^-}/f_{X^-}(0)$, as function of Triton X-114. ■(BF_4^-); ◇(NO_3^-); ▽(ClO_4^-); □(Br^-); ○(I^-); △(SCN^-). $[\text{X}_i^-] = 0.1 \text{ mM}$.

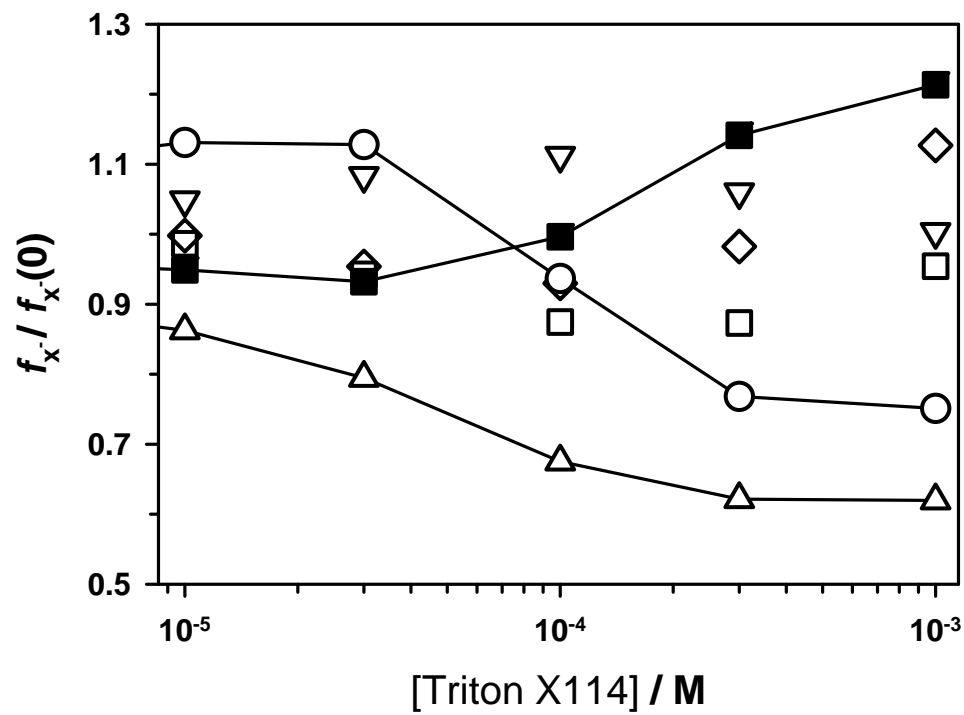


Figure 2.8. Symbols: Normalized anion affinities, f_{X^-} , as function of sodium dodecylsulfate (SDS) concentration. ■(BF_4^-); ◇(NO_3^-); ▽(ClO_4^-); □(Br^-); ○(I^-); △(SCN^-). $[\text{X}_i^-] = 0.1 \text{ mM}$.

